Preparation of β-CuGaO2 thin films by ion-exchange of β-NaGaO2 film fabricated by a solgel method

Thomas Fix, Jean-Luc Rehspringer, Stéphane Roques, Abdelilah Slaoui

Preparation of β-$CuGaO_2$ thin films by ion-exchange of β-$NaGaO_2$ film fabricated by a solgel method

T. Fix[1*], J.-L. Rehspringer[2], S. Roques[1], A. Slaoui[1]

[1] ICube laboratory, CNRS and Université de Strasbourg, 23 rue du Loess, 67037 Strasbourg, France

[2] Institut de Physique et Chimie des Matériaux de Strasbourg (IPCMS), UMR 7504 CNRS and Université de Strasbourg, 23 rue du Loess, BP 43, F-67034 Strasbourg Cedex 2, France

* Corresponding author. Tel.: +33 388106334, Fax +33 388106548. E-mail address: tfix@unistra.fr

Abstract

β-$CuGaO_2$ is a wurtzite-derived phase that is promising for ferroelectric and photovoltaic applications. Its bandgap measured in the form of powders is about 1.5 eV and is direct according to density functional theory calculations, making it an appropriate solar light absorber. In this work, we describe our attempts to grow this complex phase by pulsed laser deposition (PLD) that resulted in growing mostly $CuGa_2O_4$ on various crystal substrates such as $SrTiO_3$ (STO), Al_2O_3 (ALO), ZnO and ZrO_2:Y (9.5 mol%Y_2O_3) (YSZ). In contrast, β-$CuGaO_2$ is obtained using ion-exchange of β-$NaGaO_2$ film fabricated with a cost-efficient spin coating by solgel method, on substrates composed of a SiN film on c-Si (001) wafer. The potential of the different films obtained is discussed in view of photovoltaic applications using Surface Photovoltage under white light and Surface Photovoltage spectroscopy. While we show that

β-$CuGaO_2$ is a suitable photon absorber we conclude that the fact that the films are discontinuous is detrimental for electronic transport and additional dopants must be inserted in this material to promote its optoelectronic properties and charge carrier transport.

Keywords: thin films; oxide materials; photovoltaics; photon absorber

Introduction

Inorganic thin film photovoltaics is mainly based on cadmium telluride, amorphous silicon and copper indium gallium sulfide/selenide (CIGSSe). Recently, hybrid perovskites have emerged with efficiencies rivalling the record efficiencies of Si. However they still suffer from stability, reliability, scale up and toxicity issues, although progress is fast. An alternative could be offered by inorganic oxide absorbers. Two materials share the record laboratory conversion efficiency of 8.1 % for oxide solar cells: cuprous oxide Cu_2O and the double perovskite Bi_2FeCrO_6 [1-5]. The former has a bandgap of 2.1 eV which is not optimal as the ideal bandgap for a single bandgap solar cell is about 1.3 eV for the solar spectrum [1]. The latter, Bi_2FeCrO_6, is based on the concept of ferroelectric solar cells which do not require a *pn* junction as the ferroelectric behavior is responsible for carrier separation and migration towards the contacts [4]. Here we investigate an emergent material in the form of thin film, β-$CuGaO_2$. It contains, as in CIGS, copper and gallium but the scarce indium and toxic S/Se elements are not present. Its bandgap measured in the form of powders is 1.47 eV and is direct according to density functional theory calculations, making it an appropriate solar light absorber [6]. The ferroelectric properties are thought to be remarkable with a computed remanence polarisation of 84 µC/cm², surpassing $BiFeO_3$ single-crystal (~60 µC/cm² along <100>) and comparable to $LiNbO_3$ (~80 µC/cm²) and $PbTiO_3$ (~90 µc/cm²) [7]. Thus several studies pointed out this material as an excellent candidate for ferroelectric solar cells [6,7]. β-$CuGaO_2$ has a wurtzite structure which is not the most stable oxide compared to Cu_2O, CuO and α-$CuGaO_2$ [8]. Therefore β-$CuGaO_2$ powders have been discovered by fabricating first β-$NaGaO_2$ powders and by further substitution of Na by Cu [6]. The only report on β-$CuGaO_2$ thin films is using a similar method, by first depositing β-$NaGaO_2$ films by sputtering and then by substitution of Na by Cu using CuCl vapour [9]. The fabrication of β-$NaGaO_2$ films by sputtering is not very convenient because of Na contamination of the chamber and hygroscopy of the β-$NaGaO_2$ compound. In this work, we investigate the direct growth of thin film β-$CuGaO_2$ by pulsed laser deposition (PLD). We also present an alternative original method to obtain β-$CuGaO_2$ using ion-exchange of β-$NaGaO_2$ film

fabricated with a cost-efficient spin coating by solgel method. We studied the potential of the grown films using the surface photovoltage (SPV) technique.

1. Experimental procedure

PLD fabrication

The substrates used for PLD deposition were $SrTiO_3$ (001) and (110) (STO), Al_2O_3 (0001) (ALO), ZnO (0001) and ZrO_2:Y (9.5 mol%Y_2O_3) (111) YSZ from Crystal GmbH. The PLD process was performed using a KrF laser (248 nm) with a 10 Hz repetition rate and a laser fluence of around 1-2 J/cm^2 (36000 pulses). The depositions were carried out at 700-800°C under an oxygen pressure of 10^{-2} mbar. The films were naturally cooled down under the same atmosphere until room temperature. Around 20 samples were deposited by PLD for the study. The $CuGaO_2$ target was made by mixing CuO (99.995 % purity, Alfa Aesar) and Ga_2O_3 (99.999 % purity, Alfa Aesar) powders in the required quantities, pressing into a pellet with a vertical pressure die and then with a cold isostatic press system (MIT Corporation YLJ-CIP-500M-30) at 460 Mpa actual pressure. The obtained pellet was then calcinated at 800°C for 3 h in air and used as a target.

Solgel fabrication

The β-$NaGaO_2$ films were prepared as follows. First, 5 g of gallium (III) nitrate hydrate (99.9 % purity, Sigma Aldrich) is poured in deionised water (~50 ml) together with 10 g of citric acid (99 %, Sigma Aldrich) and 10 g of ethylene glycol (> 99 %, Sigma Aldrich). The solution is heated while stirring with a magnetic bar until most of the excess of water is evaporated while releasing NO_2 gas. The obtained viscous and transparent solution is completed with 1.19665 g of sodium citrate tribasic dihydrate (≥ 99.0 %, Fluka). A part of the obtained paste was heated in a furnace at 700 °C for 1 h in air. The resulting white powder was analyzed by XRD which provided evidence of a β-$NaGaO_2$ phase.

Next, silicon nitride was deposited on 1-5 Ω·cm p-type (B-doped) c-Si (001) wafer by plasma-enhanced chemical vapour deposition (PECVD, Roth & Rau MicroSys 400 reactor). The Si substrates were etched

with HF (10% vol) before pumping (deoxidation). A SiN thickness of 157 nm was measured by spectroscopic ellipsometry. These films were then used as substrates for spin-coating with the aforementioned paste. The spin coating parameters were 2000 rpm speed, 2000 rpm/s acceleration and 30 min spin coating duration. The spin-coated samples were then heated in air at 700°C for 1 h with a heating rate of 3.3 °C/min and natural cooling. When the furnace cooldown reached ~40 °C the obtained β-$NaGaO_2$ films were placed in an alumina crucible and sprinkled with copper (I) chloride powder (purity ≥ 99 %, Sigma Aldrich). The powder was gently pressed onto the films. The crucible and samples were quickly inserted in a quartz tube and pumped until reaching a vacuum better than 1.5×10^{-6} mbar. A furnace was placed around the quartz tube and set at 250°C for 17 h under dynamic vacuum. The final pressure after cooldown was 5×10^{-7} mbar. The samples were then rinsed with deionised water and dried under Ar gas flow.

Film characterization

Films grown by PLD on crystal substrates were investigated using at room temperature a Rigaku SmartLab diffractometer equipped with a monochromatic source delivering a Cu $K_{\alpha1}$ incident beam (45 kV, 200 mA, 0.154056 nm). Films grown by the solgel method were investigated with a Bruker D8 Discover X-ray diffractometer with Cu $K_{\alpha1}$ radiation (40 kV, 40 mA, 0.154056 nm) at room temperature.

The optical properties and thickness of the films were investigated by spectroscopic ellipsometry using a HORIBA Uvisel Lt M200 FGMS (210–880 nm) apparatus. The dispersion formula for SiN and β-$CuGaO_2$ are based on the classical and triple Tauc-Lorentz models respectively [10]. The goodness-of-fit values (Chi Square χ^2) was 4.5 for a β-$CuGaO_2$ film thickness of around 240 nm. Photoluminescence (PL) measurements were performed using a Horiba LabRAM ARAMIS spectrometer with 532 nm laser excitation (HeNe).

The surface of the films was investigated using atomic force microscopy (AFM) with a NT-MDT Smena B AFM in tapping mode. Scanning electron microscopy (SEM) was performed with a JEOL 6700F and a JEOL JSM-IT200LA apparatus and the stoichiometry was checked by Energy-dispersive X-ray spectroscopy (EDS). Kelvin Probe (KP) and Surface PhotoVoltage (SPV) measurements were performed with a single point Kelvin Probe system (KP Technology KP020) with a 2 mm diameter gold tip, and using either a halogen source with calibrated illumination for white light SPV or a GR50-605 (Thorlabs) monochromator of 600 g/mm grating for Surface Photovoltage Spectroscopy (SPS) mode.

2. Results and discussion

PLD growth

Knowing that there is a small lattice mismatch of β-$CuGaO_2$ lattice with ZnO [8], we attempted to deposit β-$CuGaO_2$ by PLD using substrates that may provide an epitaxial relationship with β-$CuGaO_2$, namely STO (001) and (110), ALO (0001), ZnO (0001) and YSZ (111). The original method of fabrication of β-$CuGaO_2$ powders uses a two-step method by first fabricating β-$NaGaO_2$ and then substituting Na by Cu [8]. This is because β-$CuGaO_2$ cannot be formed using conventional solid state synthesis from oxide powders as it is not the most thermodynamically stable phase. However, PLD is known for enabling the fabrication of metastable phases that would form from the plasma material onto the substrate. Furthermore, a principle called epitaxial stabilization helps synthetizing complex material by using an appropriate substrate playing the role of a template to promote the right phase formation. This has been demonstrated for example with h-$TbMnO_3$ thin film fabrication while orthorhombic $TbMnO_3$ is the most stable phase [11,12]. Films grown on STO (110) using a $CuGaO_2$-stoichiometry target provided $CuGa_2O_4$ films with the following orientation $CuGa_2O_4$ (220)//STO(110) while films grown on ALO (0001) provided $CuGa_2O_4$ films with $CuGa_2O_4$ (222)//ALO(0001) orientation (Figure 1). This means that clearly the substrate has an influence on film growth, although the desired β-$CuGaO_2$ phase was not obtained. $CuGa_2O_4$ is reported in [13] to grow along the (111) orientation on ALO (0001) substrate. This is because the observation along the [111] direction of the cubic $CuGa_2O_4$ lattice is a

hexagonal sampling lattice matching with the hexagonal lattice of ALO [13]. As well $CuGa_2O_4$ grows in the (220) direction on STO (110) because of the lattice match in plane between STO (001) and $CuGa_2O_4$ (002) and between STO $(1\bar{1}0)$ and $CuGa_2O_4$ $(2\bar{2}0)$. EDS analysis (Figure S1 of the Supplementary Information (SI)) indicated a stoichiometry of Cu:Ga:O of 1:0.85:1.87 indicating that while the chemical composition of the films is close to $CuGaO_2$, the structural crystallized phase is $CuGa_2O_4$. This means that the deposition is rather congruent, preserving the chemical stoichiometry from the target to the film, which was an incentive to perform further depositions using alternative substrates. The evaluation of $CuGa_2O_4$ films grown on STO (110) by SPV showed that these films provide a strong photoresponse, nearly as good under white light as 1-5 Ω·cm p-type c-Si wafers (Figure S2a). SPS was performed on the same sample and shows that the photoresponse originates from photons below 600 nm, indicating that the electronic bandgap is above 2 eV (Figure S2b).

Further crystal substrates were used for film growth. Unfortunately, films grown on ZnO (0001) and YSZ (111) gave $CuGa_2O_4$ (222)//ZnO (0002) and $CuGa_2O_4$ (222)//YSZ (111) orientations respectively (Figure S3 of SI). In the latter film two XRD peaks could be also attributed to a delafossite α-$CuGaO_2$ phase (rhombohedral R-3m (166), ICDD 04-010-0383). The case of STO (001) substrate gives a similar outcome (Figure S3). As pointed out in [8,9], deposition of β-$CuGaO_2$ is difficult because β-$CuGaO_2$ transforms into stable α-$CuGaO_2$ at temperatures higher than 500°C under low O_2 atmosphere and decomposes in CuO and $CuGa_2O_4$ at temperatures higher than 300°C under O_2 atmosphere. A phase diagram of Cu-Ga-O is proposed in [14,15] but again should be used with care due to the non-thermodynamic equilibrium of PLD deposition. Attempts to obtain the right β-$CuGaO_2$ films by reducing the O_2 pressure from 10^{-2} mbar to 10^{-3} or 10^{-4} mbar were unsuccessful. A fine tuning of both the deposition temperature and the oxygen pressure could help promote the α-$CuGaO_2$ phase as evidenced in [16] but this strategy was not followed here as only the β-$CuGaO_2$ phase is sought. Instead, we decided to investigate fabrication of β-$CuGaO_2$ thin films by ion-exchange of β-$NaGaO_2$ film fabricated with spin coating by a solgel method.

Fabrication by solgel

Solgel fabrication of thin films is an inexpensive scalable method for fabricating oxides. In some cases this method provides better results than physical deposition, as in the case of $LaVO_3$ [17]. Knowing that a simple mixture of β-$CuGaO_2$ precursors in a traditional solgel experiment would not work for the aforementioned reasons, we decided to get inspired from the two-step fabrication in the way that the first β-$CuGaO_2$ powders were produced: first the fabrication of a β-$NaGaO_2$ film and second the substitution of Na by Cu [6]. As described in the experimental section, a precursor paste for β-$NaGaO_2$ was produced and spin coated on SiN//c-Si substrates. The spin coated samples were then heated in a furnace and resulted in the formation of β-$NaGaO_2$ film as shown in Figure 2 and evidenced by XRD in Figure 3a). In contrast to the current method, the introduction of sodium citrate tribasic dihydrate at the same time as gallium (III) nitrate hydrate in water followed by heating does not lead to the right β-$NaGaO_2$ phase. It should also be noted that β-$NaGaO_2$ films degrade within few hours in air so that they need to be processed rapidly with the next step. A second remark is that spin coating and annealing on c-Si substrates without the SiN layer did not enable to obtain the β-$NaGaO_2$ phase. It is believed that the SiN film acts as a barrier for Na diffusion into the substrate during the annealing at 700 °C. The next step was to sprinkle CuCl powder on the β-$NaGaO_2$ sample, pump the sample under dynamic vacuum and heat at 250°C for 17 hours. It was found that a starting vacuum before heating of 8×10^{-6} mbar was ineffective to form the β-$CuGaO_2$ phase as CuCl was oxidized, while a starting vacuum better than 1.5×10^{-6} mbar was satisfactory. The sample was naturally cooled down to room temperature before opening the furnace tube. The films obtained in this way present the right β-$NaGaO_2$ phase as evidenced by XRD (Figure 3b). The composition was analyzed by EDS and provided a $CuGa_{1.06}O_y$ stoichiometry, very close to the perfect composition of β-$CuGaO_2$ (Figure S4). Traces of Cl originating from the CuCl step were found, which could be further reduced by acetonitrile and ethanol washing as proposed in [9]. Although the films look visually uniform and flat (Figure 2), SEM performed on the samples shows that the films are discontinuous (Figure 4). Much smaller cracks were also observed in [9] and originate from lattice shrinkage during the ion exchange from β-$NaGaO_2$ thin film

177 to β-$CuGaO_2$ thin film. AFM performed on the samples reveals a root-mean-square (RMS) roughness
178 in the 300 nm range (Figure S5) which is rather high compared to films obtained by physical methods.
179 Also the films look much darker than the initial SiN//c-Si substrates; and their optical properties were
180 further investigated by spectroscopic ellipsometry. A thickness of about 240 nm and a bandgap of
181 about 1.91 eV were found (Figure 5). Such a high film thickness was obtained because the precursor
182 paste at step 1 was very viscous. The absorption coefficient was in the 10^5 cm^{-1} range in the 2-6 eV
183 region, which is at 600 nm more than an order of magnitude higher than diamond Silicon. The optical
184 parameters n and k were also determined (Figure S6). The optical properties were further investigated
185 by PL (Figure S7). No sharp PL peak is observed around the bandgap or anywhere in the β-$CuGaO_2$
186 spectrum. The presence of a sharp peak would have indicated a high quality direct bandgap material.

187 We now focus in the electrical properties of the films. The work function was measured with the Kelvin
188 probe system and was found to be in the 5.1-5.3 eV range. The value should be used with caution as
189 the surface state of β-$CuGaO_2$ film is uncertain. Still, this value can be compared to the delafossite α-
190 $CuGaO_2$ reported value of 4.90 eV [18]. Unfortunately, no Hall effect could be performed because the
191 samples were too insulating for the setup. This could be caused by the fact that the films are
192 discontinuous as observed in Figure 4. To overcome these carrier transport limitations, we attempted
193 to produce β-$CuGaO_2$ on conductive substrates. Because indium tin oxide (ITO) films would not
194 withstand an annealing temperature of 700 °C, we opted for 50 nm thick Pt layers sputtered on quartz
195 substrates and we followed the aforementioned procedure to produce β-$CuGaO_2$ films. While the right
196 β-$CuGaO_2$ phase could be obtained again, the surface of the films was severely damaged as shown in
197 Figure S8. The adherence of β-$CuGaO_2$ on Pt is low and thus Pt areas are exposed after detachment of
198 β-$CuGaO_2$ fragments. To further investigate the potential of the β-$CuGaO_2$ films produced, we
199 performed SPV measurements on films both on SiN//c-Si and Pt//quartz. Unfortunately no SPV signal
200 could be extracted as shown in Figure S9. We believe that the main limitation for β-$CuGaO_2$ as a
201 photovoltaic absorber is that the carrier transport is poor, probably due to the discontinuous nature
202 of the film, although the optical properties are promising. A possible way to go forward would be to

study electrical doping of β-$CuGaO_2$, which would be simple to adapt from the proposed solgel procedure.

Conclusions

In summary, we first have attempted to grow β-$CuGaO_2$ by PLD. This was unsuccessful and the best films produced on various crystal substrates were $CuGa_2O_4$. Some of these films provided high SPV response and SPS spectroscopy indicates that this response is rather generated by photons below 600 nm wavelength. In contrast, β-$CuGaO_2$ films were produced with an inexpensive ion-exchange of β-$NaGaO_2$ fabricated with spin coating by a solgel method which delivered well crystallized but discontinuous films. Although the optical properties obtained are interesting, further effort is necessary to obtain smoother films and improve carrier transport of β-$CuGaO_2$ by doping the material so that better optoelectronic response can be obtained in the future.

Figure 1 XRD θ-2θ patterns of films grown by PLD on a) STO (110) b) ALO (0001) from a $CuGaO_2$ target, and of the $CuGa_2O_4$ ICDD reference

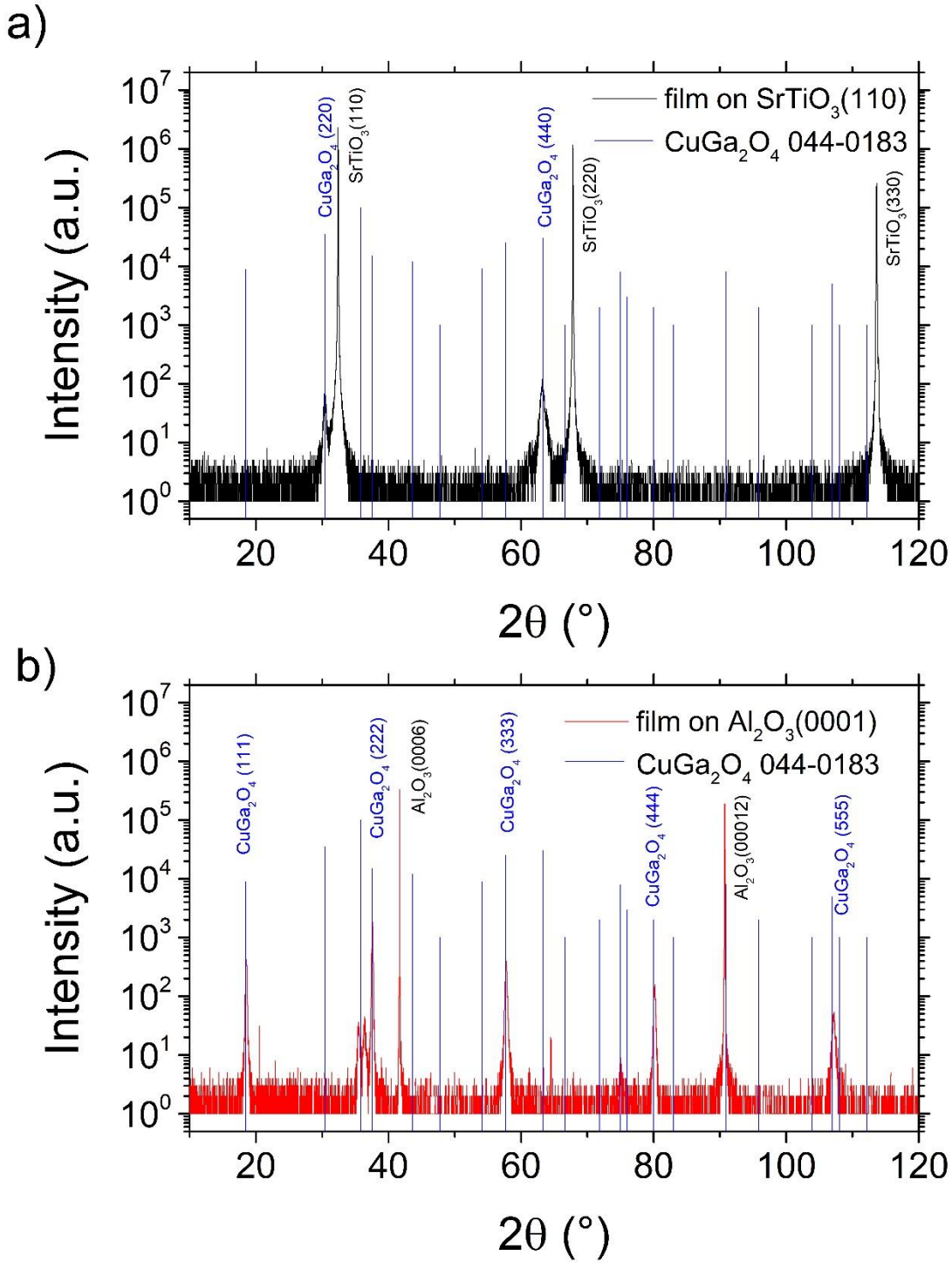

220 **Figure 2** Top-view photographs showing the fabrication of β-$CuGaO_2$ film obtained using ion-

221 exchange of β-$NaGaO_2$ film fabricated with spin coating by solgel method on c-Si//SiN

Substrate as grown: SiN (157 nm)//c-Si	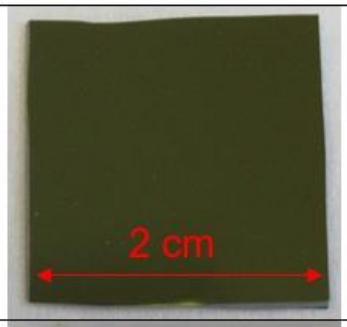
After annealing 700°C 1h $NaGaO_2$/SiN//c-Si	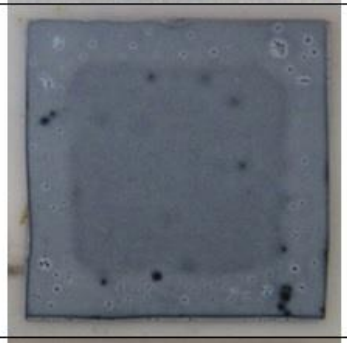
CuCl powder on sample CuCl/$NaGaO_2$/SiN//c-Si	
After 250°C 17h in vacuum CuCl/$NaGaO_2$/SiN//c-Si	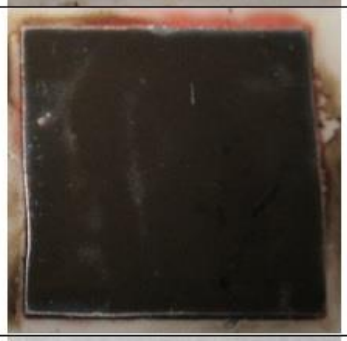
β-$CuGaO_2$/SiN//c-Si	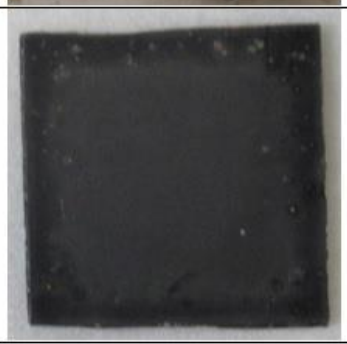

222

223 **Figure 3** XRD θ-2θ patterns showing the β-$NaGaO_2$, and β-$CuGaO_2$ films obtained using ion-exchange

224 of β-$NaGaO_2$ film fabricated with spin coating by solgel method, and the ICDD references

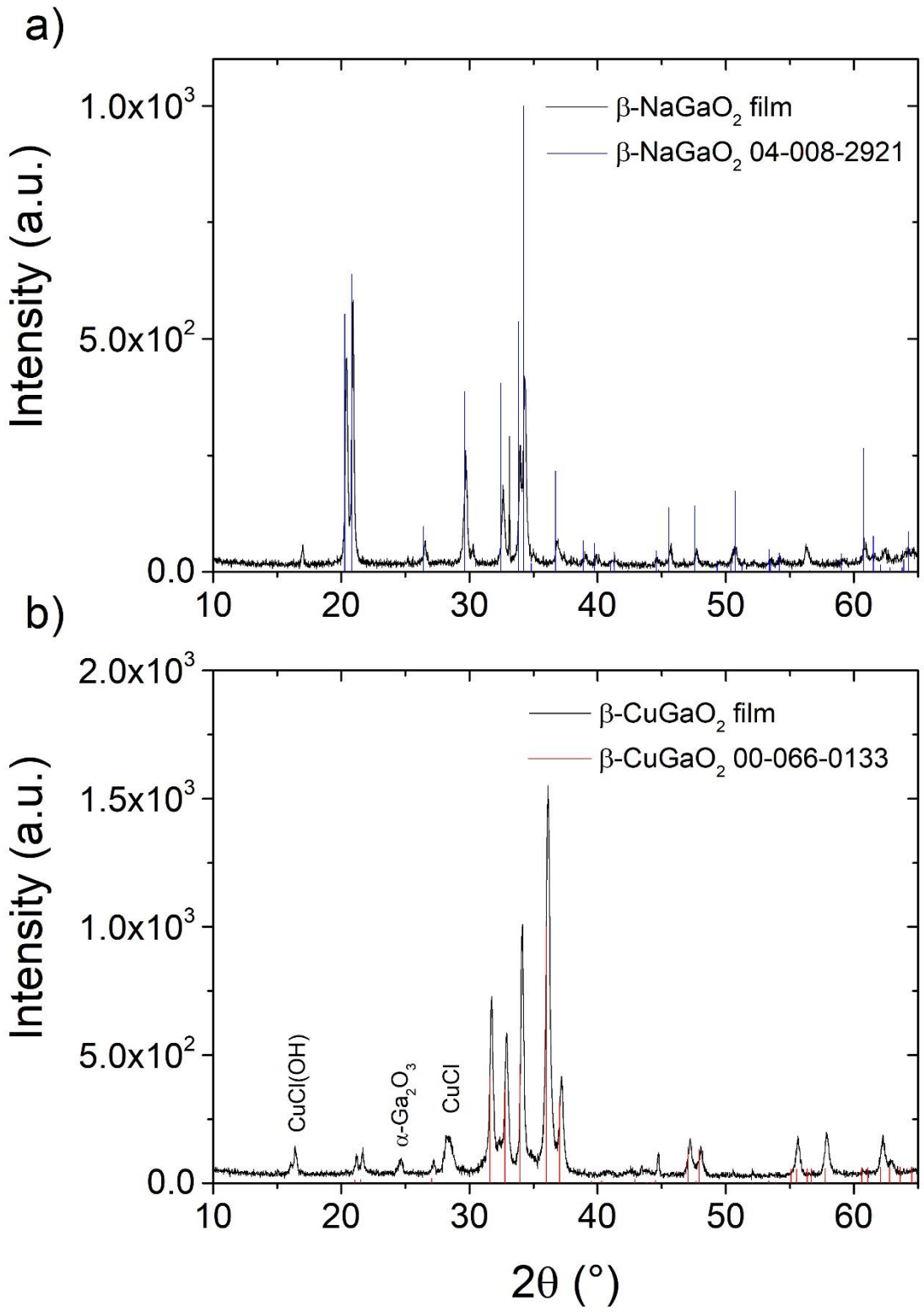

225

226

Figure 4: SEM top view of a β-$CuGaO_2$ film obtained using ion-exchange of β-$NaGaO_2$ film fabricated with spin coating by solgel method

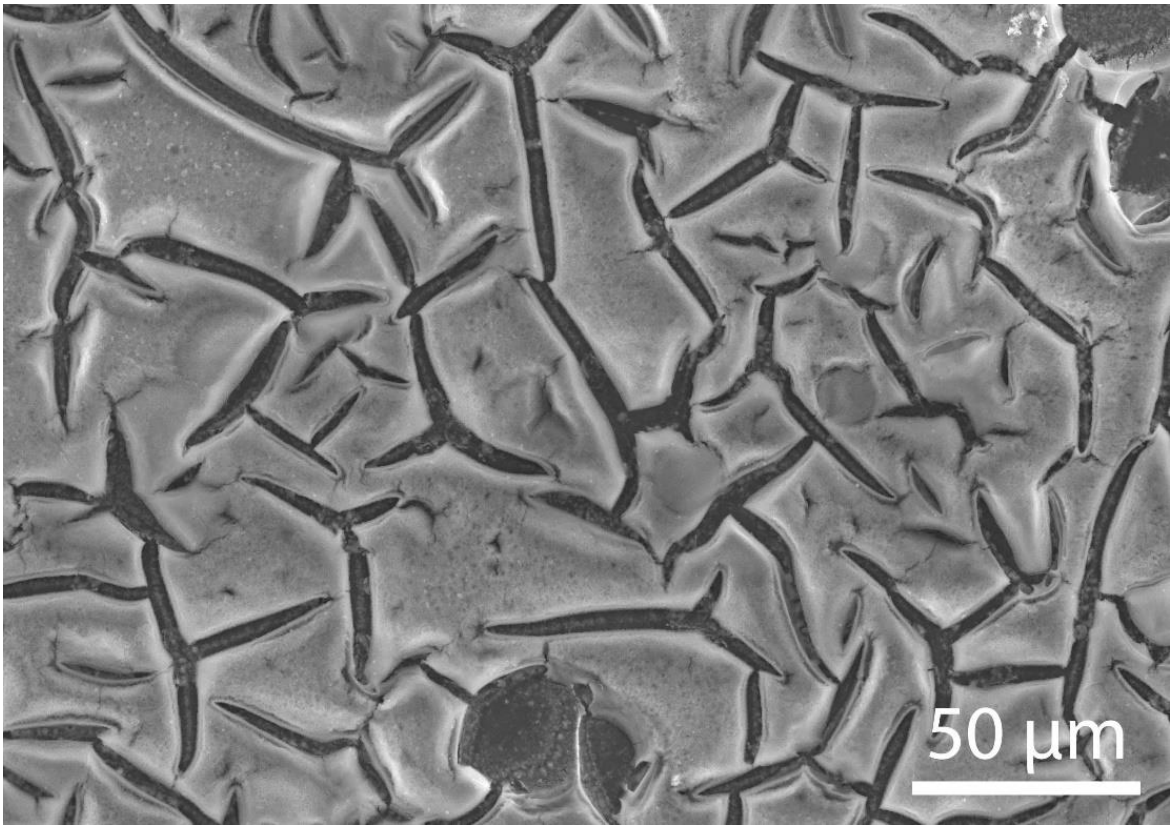

Figure 5 Absorption coefficient determined by spectroscopic ellipsometry for a β-$CuGaO_2$ sample, obtained using ion-exchange of β-$NaGaO_2$ film fabricated with spin coating by solgel method on c-Si//SiN. The reference for diamond silicon is taken from [19]

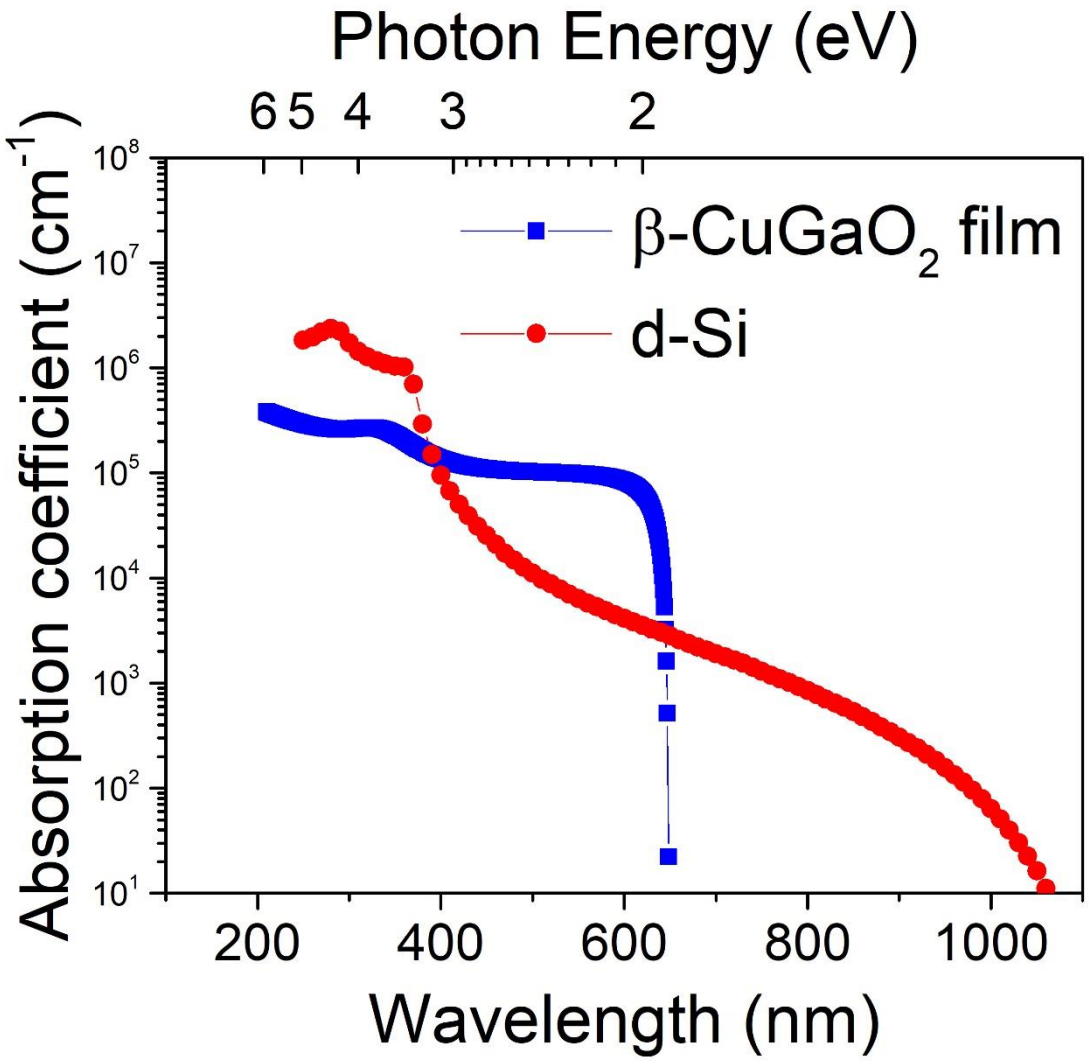

References

1. T. Fix, in *Advanced Micro- and Nanomaterials for Photovoltaics*, edited by D. Ginley and T. Fix (Elsevier Science Bv, Amsterdam, 2019), p. 19.
2. A. Quattropani, D. Stoeffler, T. Fix, G. Schmerber, M. Lenertz, G. Versini, J. L. Rehspringer, A. Slaoui, A. Dinia, and S. Cois, J. Phys. Chem. C **122,** 1070 (2018). https://doi.org/10.1021/acs.jpcc.7b10622
3. A. Quattropani, A. S. Makhort, M. V. Rastei, G. Versini, G. Schmerber, S. Barre, A. Dinia, A. Slaoui, J. L. Rehspringer, T. Fix, S. Colis, and B. Kundys, Nanoscale **10,** 13761 (2018). https://doi.org/10.1039/c8nr03137a
4. R. Nechache, C. Harnagea, S. Li, L. Cardenas, W. Huang, J. Chakrabartty, and F. Rosei, Nat. Photonics **9,** 61 (2015). https://doi.org/10.1038/nphoton.2014.255
5. T. Minami, Y. Nishi, and T. Miyata, Appl. Phys. Express **9** (2016). https://doi.org/10.7567/apex.9.052301
6. T. Omata, H. Nagatani, I. Suzuki, M. Kita, H. Yanagi, and N. Ohashi, Journal of the American Chemical Society **136,** 3378 (2014). https://doi.org/10.1021/ja501614n
7. S. Song, D. Kim, H. M. Jang, B. C. Yeo, S. S. Han, C. S. Kim, and J. F. Scott, Chem. Mater. **29,** 7596 (2017). https://doi.org/10.1021/acs.chemmater.7b03141
8. H. Nagatani, I. Suzuki, M. Kita, M. Tanaka, Y. Katsuya, O. Sakata, S. Miyoshi, S. Yamaguchi, and T. Omata, Inorg. Chem. **54,** 1698 (2015). https://doi.org/10.1021/ic502659e
9. I. Suzuki, H. Nagatani, M. Kita, and T. Omata, Appl. Phys. Express **10,** 4 (2017). https://doi.org/10.7567/apex.10.095501
10. F. Wooten, *Optical Properties of Solids* (Elsevier Inc., 1972).
11. T. Fix, G. Schmerber, J. L. Rehspringer, M. V. Rastei, S. Roques, J. Bartringer, and A. Slaoui, J. Alloys Compd. **883,** 6 (2021). https://doi.org/10.1016/j.jallcom.2021.160922
12. J. H. Lee, P. Murugavel, H. Ryu, D. Lee, J. Y. Jo, J. W. Kim, H. J. Kim, K. H. Kim, Y. Jo, M. H. Jung, Y. H. Oh, Y. W. Kim, J. G. Yoon, J. S. Chung, and T. W. Noh, Adv. Mater. **18,** 3125 (2006). https://doi.org/10.1002/adma.200601621
13. H. L. Wei, Z. W. Chen, Z. P. Wu, W. Cui, Y. Q. Huang, and W. H. Tang, Aip Advances **7,** 7 (2017). https://doi.org/10.1063/1.5009032
14. V. Varadarajan and D. P. Norton, Appl. Phys. A: Mater. Sci. Process. **85,** 117 (2006). https://doi.org/10.1007/s00339-006-3667-0
15. R. B. Gall and D. P. Cann, in *High temperature phase equieliebria in the Cu2O-Ga2O3-In2O3 system*, Cocoa Beach, Fl, 2003 (Amer Ceramic Soc), p. 143.
16. T. Mine, H. Yanagi, K. Nomura, T. Kamiya, M. Hirano, and H. Hosono, Thin Solid Films **516,** 5790 (2008). https://doi.org/10.1016/j.tsf.2007.10.072
17. M. Jellite, J. L. Rehspringer, M. A. Fazio, D. Muller, G. Schmerber, G. Ferblantier, S. Colis, A. Dinia, M. Sugiyama, A. Slaoui, D. Cavalcoli, and T. Fix, Sol. Energy **162,** 1 (2018). https://doi.org/10.1016/j.solener.2017.12.061
18. J. Wang, V. Ibarra, D. Barrera, L. Xu, Y. J. Lee, and J. Hsu, J. Phys. Chem. Lett. **6,** 1071 (2015). https://doi.org/10.1021/acs.jpclett.5b00236
19. M. A. Green and M. J. Keevers, Progr. Photovolt. **3,** 189 (1995). https://doi.org/https://doi.org/10.1002/pip.4670030303

Statements and Declarations

Funding

This work has been partially funded by the CNRS Energy unit (Cellule Energie) through the project CIGALE-PV and by the IdEx University of Strasbourg.

Declaration of Competing Interest

The authors declare that they have no known competing financial interests or personal relationships that could have appeared to influence the work reported in this paper.